NASA/TM—2019–220332

# TESS Data Release Notes:
## Sector 13, DR18

*Michael M. Fausnaugh, Christopher J. Burke*
*Kavli Institute for Astrophysics and Space Science, Massachusetts Institute of Technology, Cambridge, Massachusetts*

*Douglas A. Caldwell*
*SETI Institute, Mountain View, California*

*Jon M. Jenkins*
*NASA Ames Research Center, Moffett Field, California*

*Jeffrey C. Smith, Joseph D. Twicken*
*SETI Institute, Mountain View, California*

*Roland Vanderspek*
*Kavli Institute for Astrophysics and Space Science, Massachusetts Institute of Technology, Cambridge, Massachusetts*

*John P. Doty*
*Noqsi Aerospace Ltd, Billerica, Massachusetts*

*Eric B. Ting*
*Ames Research Center, Moffett Field, California*

*Joel S. Villasenor*
*Kavli Institute for Astrophysics and Space Science, Massachusetts Institute of Technology, Cambridge, Massachusetts*

**August 14, 2019**

## Acknowledgements

These Data Release Notes provide information on the processing and export of data from the Transiting Exoplanet Survey Satellite (TESS). The data products included in this data release are full frame images (FFIs), target pixel files, light curve files, collateral pixel files, cotrending basis vectors (CBVs), and Data Validation (DV) reports, time series, and associated xml files.

These data products were generated by the TESS Science Processing Operations Center (SPOC, Jenkins et al., 2016) at NASA Ames Research Center from data collected by the TESS instrument, which is managed by the TESS Payload Operations Center (POC) at Massachusetts Institute of Technology (MIT). The format and content of these data products are documented in the Science Data Products Description Document (SDPDD)[1]. The SPOC science algorithms are based heavily on those of the Kepler Mission science pipeline, and are described in the Kepler Data Processing Handbook (Jenkins, 2017).[2] The Data Validation algorithms are documented in Twicken et al. (2018) and Li et al. (2019). The TESS Instrument Handbook (Vanderspek et al., 2018) contains more information about the TESS instrument design, detector layout, data properties, and mission operations.

The TESS Mission is funded by NASA's Science Mission Directorate.


This report is available in electronic form at
https://archive.stsci.edu/tess/

[1]https://archive.stsci.edu/missions/tess/doc/EXP-TESS-ARC-ICD-TM-0014.pdf

[2]https://archive.stsci.edu/kepler/manuals/KSCI-19081-002-KDPH.pdf

# 1 Observations

TESS Sector 13 observations include physical orbits 33 and 34 of the spacecraft around the Earth. Data collection was paused for 0.93 days during perigee passage while downloading data. In total, there are 27.51 days of science data collected in Sector 13.

Table 1: Sector 13 Observation times

| | UTC | TJD[a] | Cadence # |
|---|---|---|---|
| Orbit 33 start | 2019-06-19 09:55:30 | 1653.91505 | 307051 |
| Orbit 33 end | 2019-07-03 04:31:30 | 1667.69004 | 316969 |
| Orbit 34 start | 2019-07-04 02:49:30 | 1668.61921 | 317638 |
| Orbit 34 end | 2019-07-17 20:31:29 | 1682.35670 | 327529 |

[a] TJD = TESS JD = JD - 2,457,000.0

The spacecraft was pointing at RA (J2000): 298.6671°; Dec (J2000): −76.3281°; Roll: −161.0622°. Two-minute cadence data were collected for 20,000 targets, and full frame images were collected every 30 minutes. See the TESS project Sector 13 observation page[3] for the coordinates of the spacecraft pointing and center field-of-view of each camera, as well as the detailed target list. Fields-of-view for each camera and the Guest Investigator two-minute target list can be found at the TESS Guest Investigator Office observations status page[4].

## 1.1 Notes on Individual Targets

Three very bright stars (Tmag $\lesssim$ 1.8) with large pixel stamps were not processed in the photometric pipeline. Target pixel files with raw data are provided, but no light curves were produced. The affected TIC IDs are 38877693, 49231061, 57334718.

Two target stars (300015238 and 300015239) are blended with each other—the contaminating flux for these objects is very large, and the resulting photometry for such targets is expected to be unreliable.

Two bright (Tmag $\lesssim$ 1.6), saturated, bleeding targets (238196512 and 384196595) had selected pixel stamps that did not fully capture the bleed trails.

## 1.2 Spacecraft Pointing and Momentum dumps

The reaction wheel speeds were reset with momentum dumps every 3.375 days. Figure 1 summarizes the pointing performance over the course of the sector based on Fine Pointing telemetry.

At the start of Orbit 33, the Moon was close enough to the boresight of Camera 1 that the level of scattered light would have been too high for meaningful guide star centroids to be measured in Camera 1. Therefore, guiding with Camera 1 was disabled and Camera 4 alone was used for guiding in all of orbit 33. In Orbit 34, both Camera 1 and Camera 4 were

[3] https://tess.mit.edu/observations/sector-13

[4] https://heasarc.gsfc.nasa.gov/docs/tess/status.html

used for guiding for the entire duration of the orbit. This configuration is identical to that used in Sector 12—refer to DRN 17 for a description of the effects on the spacecraft pointing performance.

Finally, a single upset event in the star trackers on the spacecraft bus resulted in a complicated interaction between the instrument quaternions and attitude control system. This interaction caused the spacecraft to fall out of fine pointing for approximately 1.25 hours from TJD 1665.2983 to 1665.3501. During this time, the spacecraft exhibited increased pointing jitter (see Figure 1). These time periods correspond to cadences 315247 to 315285, which are marked with bit 8 (Manual Exclude) data anomaly flags. This time period also spans FFIs with timestamps 2019181185930, 2019181192930, and 2019181195930, which are marked with bit 2 (Course Point) in the DQUALITY header field.

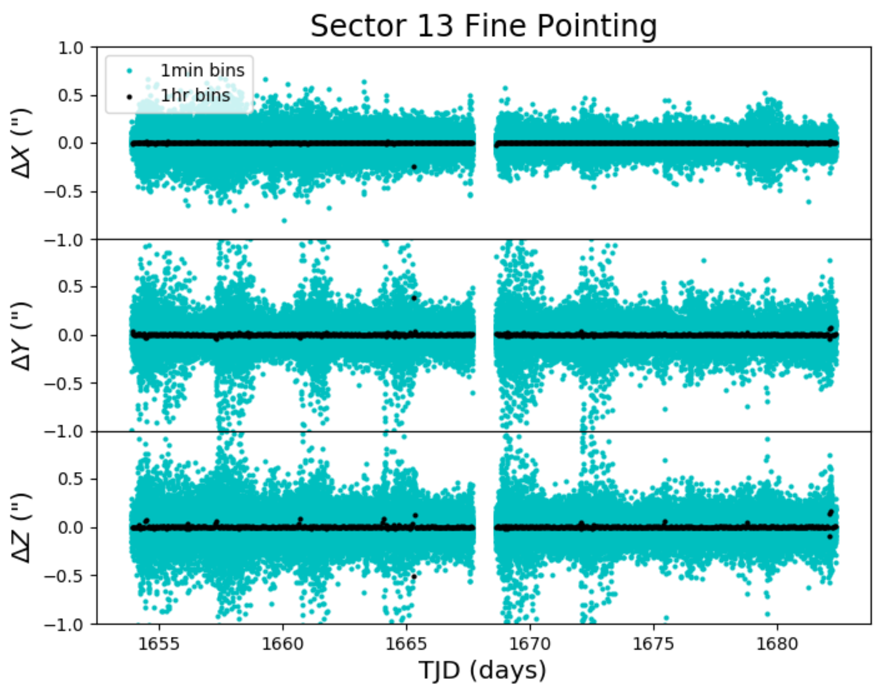


Figure 1: Guiding corrections based on spacecraft fine pointing telemetry. The delta-quaternions from each camera have been converted to spacecraft frame, binned to 1 minute and 1 hour, and averaged across cameras. Long-term trends (such as those caused by differential velocity aberration) have also been removed. The ΔX/ΔY directions represent offsets along the the detectors' rows/columns, while the ΔZ direction represents spacecraft roll.

## 1.3 Scattered Light

Figure 2 shows the median value of the background estimate for all targets on a given CCD as a function of time. Figure 3 shows the angle between each camera's boresight and the Earth or Moon—this figure can be used to identify periods affected by scattered light and the relative contributions of the Earth and Moon to the image backgrounds. In Sector 13, the main stray light features are caused by the Moon and Earth in the first three quarters of each orbit.

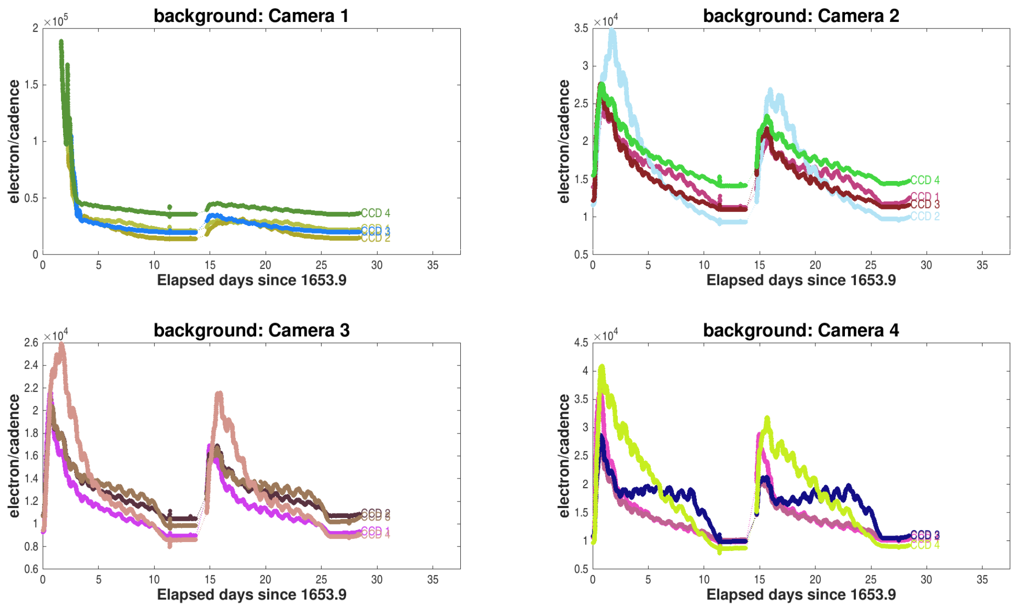


Figure 2: Median background flux across all targets on a given CCD in each camera. The changes are caused by variations in the orientation and distance of the Earth and Moon.

# 2 Data Anomaly Flags

See the SDPDD (§9) for a list of data quality flags and the associated binary values used for TESS data, and the TESS Instrument Handbook for a more detailed description of each flag.

The following flags were not used in Sector 13: bits 1, 2, 7, 9, and 11 (Attitude Tweak, Safe Mode, Cosmic Ray in Aperture, Discontinuity, Cosmic Ray in Collateral Pixel).

Cadences marked with bits 3, 4, 6, and 12 (Coarse Point, Earth Point, Reaction Wheel Desaturation Event, and Straylight) were marked based on spacecraft telemetry.

Cadences marked with bit 5 and 10 (Argabrightening Events and Impulsive Outlier) were identified by the SPOC pipeline. Bit 5 marks a sudden change in the background measurements. In practice, bit 5 flags are caused by rapidly changing glints and unstable pointing at times near momentum dumps. Bit 10 marks an outlier identified by PDC and omitted from the cotrending procedure.

Cadences marked with bit 8 (Manual Exclude) are ignored by PDC, TPS, and DV for cotrending and transit searches. In Sector 13, these cadences were identified using spacecraft telemetry from the fine pointing system. All cadences with pointing excursions >21 arcseconds (∼1 pixel) were flagged for manual exclude. As described in Section 1.2, Manual Exclude flags were also applied to the period of time affected by the single upset event in

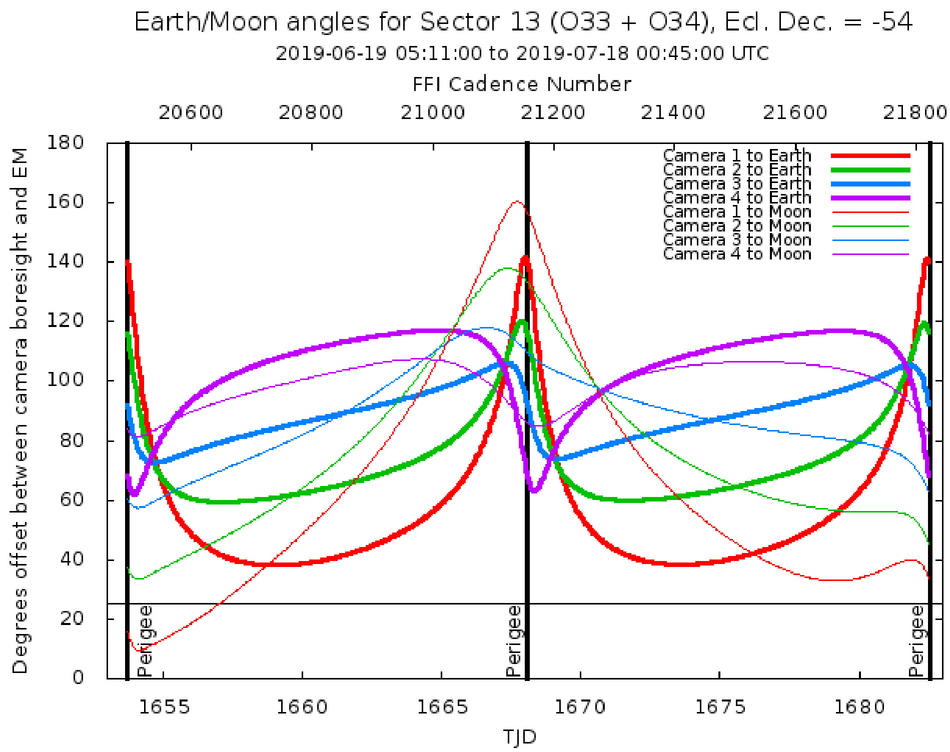


Figure 3: Angle between the four camera boresights and the Earth/Moon as a function of time. When the Earth is within $\sim 25°$ of a camera's boresight, transiting planet searches may be compromised by high levels of scattered light. At larger angles, up to $\sim 35°$, scattered light patterns and complicated structures may be visible. At yet larger angles, low level patchy features may be visible. Scattered light from the Moon is generally only noticeable below $\sim 35°$. This figure can be used to identify periods affected by scattered light and the relative contributions of the Earth and Moon to the background. However, the background intensity and locations of scattered light features depend on additional factors, such as the Earth/Moon azimuth and distance from the spacecraft.

the star trackers. See Figure 4 for an assessment of the performance of the cotrending based on the final set of manual excludes.

In addition, strong scattered light signals affected the systematic error removal in PDC and the planet search in TPS. Cadences during this time were excluded from the pipeline analysis. The time periods for these exclusions are variable per CCD, and the corresponding cadence ranges are given in Table 2. Raw and flux-calibrated (without background correction) pixels for these cadences are provided in the target pixel files, but no photometry or centroid positions were calculated. The pipeline exports do not support data quality flags on a per CCD basis, and so the QUALITY column is not marked beyond the flags described above. In Sector 13, these cadence ranges were only excluded for Camera 1 in Orbit 33.

FFIs were only marked with bits 4, 6 and 12 (Course Point, Reaction Wheel Desaturation Events and Straylight). Only one FFI is affected by each momentum dump. Note that this is the first sector with Course Point flags set outside of momentum dumps.

Table 2: Cadence ranges for data excludes due to scattered light

| Cam | CCD | Orbit 33 | Orbit 34 |
|---|---|---|---|
| 1 | 1 | 307051–308684 | ... |
| 1 | 2 | 307051–308704 | ... |
| 1 | 3 | 307051–308875 | ... |
| 1 | 4 | 307051–308242 | ... |

# 3 Anomalous Effects

## 3.1 Smear Correction Issues

The following column was impacted by bright stars in the science frame, which bleed into the upper serial register resulting in an overestimated smear correction.

- Camera 4, CCD 4, Column 1710, Star R Doradus

## 3.2 Fireflies and Fireworks

Table 3 lists all firefly and fireworks events for Sector 13. These phenomena are small, spatially extended, comet-like features in the images—created by sunlit particles in the camera FOV—that may appear one or two at a time (fireflies) or in large groups (fireworks). See the TESS Instrument Handbook for a more complete description.

Table 3: Sector Fireflies and Fireworks

| FFI Start | FFI End | Cameras | Description |
|---|---|---|---|
| 2019171035930 | 2019171042930 | 2,3 | Fireworks |
| 2019174222930 | 2019174225930 | 3 | Firefly |
| 2019183155930 | 2019183182930 | 1,2,3,4 | Fireworks |
| 2019185045930 | 2019185052930 | 3, | Fireflies |
| 2019185055930 | 2019185062930 | 2,3 | Fireflies |
| 2019188165930 | 2019188172930 | 1 | Fireflies |
| 2019189225930 | 2019190005930 | 1,2,3,4 | Fireworks |
| 2019190152930 | 2019190172930 | 1,2,3,4 | Fireworks |
| 2019191155930 | 2019191165930 | 1 | Firefly |
| 2019198082929 | 2019198085929 | 1 | Firefly |
| 2019198122929 | 2019198125929 | 3 | Firefly |
| 2019198162929 | 2019198165929 | 3 | Firefly |
| 2019198185929 | 2019198192929 | 2,3 | Firefly |

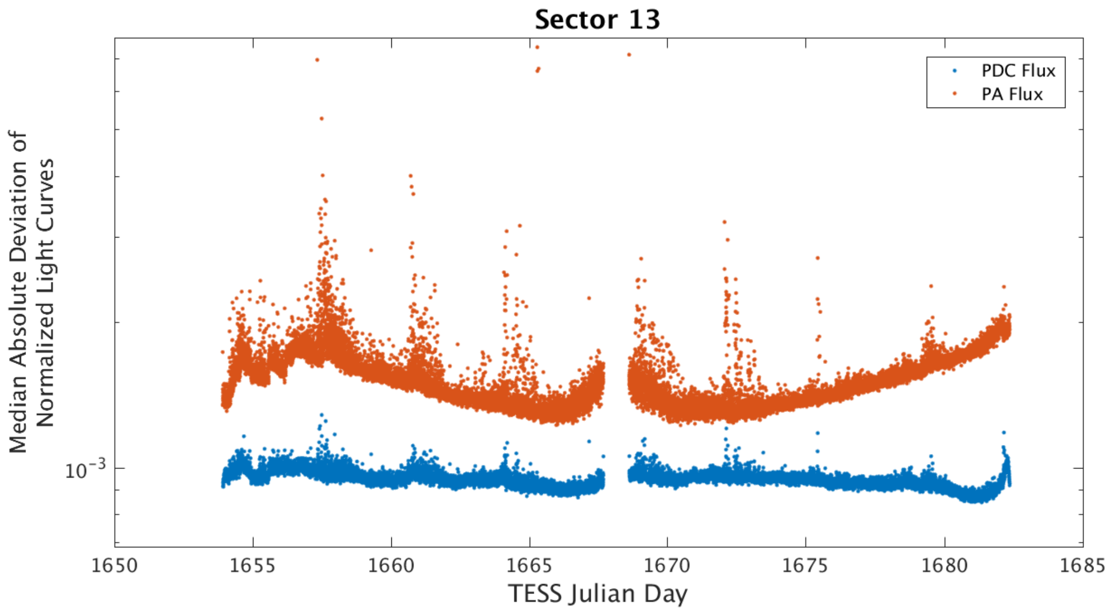


Figure 4: Median absolute deviation (MAD) for the 2-minute cadence data from Sector 13, showing the performance of the cotrending after identifying Manual Exclude data quality flags. The MAD is calculated in each cadence across stars with flux variations less than 1% for both the PA (red) and PDC (blue) light curves, where each light curve is normalized by its median flux value. The scatter in the PA light curves is much higher than that for the PDC light curves, and the outliers in the PA light curves are largely absent from the PDC light curves due to the use of the anomaly flags. Note that the first and last cadences in each orbit are treated as gaps by PDC.

# 4 Pipeline Performance and Results

## 4.1 Light Curves and Photometric Precision

Figure 5 gives the PDC goodness metrics for residual correlation and introduced noise on a scale between 0 (bad) and 1 (good). The performance of PDC is very good and generally uniform over most of the field of view. Figure 6 shows the achieved Combined Differential Photometric Precision (CDPP) at 1-hour timescales for all targets.

## 4.2 Transit Search and Data Validation

In Sector 13, the light curves of 19997 targets were subjected to the transit search in TPS. Of these, Threshold Crossing Events (TCEs) at the 7.1 $\sigma$ level were generated for 1021 targets. Cadences at the start of the first orbit were excluded from the transiting planet search due to the effects of rapidly changing scattered light and glints (see Figure 2). Planet search exclude flags were applied to cadences 307051–308875 (2.53 days) in Orbit 33.

The top panel of Figure 7 shows the distribution of orbital periods for the TPS TCEs found in Sector 13. Figure 8 shows the number of TCEs at a given cadence that exhibit a transit signal. The spikes in Figure 8 are correlated with periods of increased pointing jitter (see Figure 1).

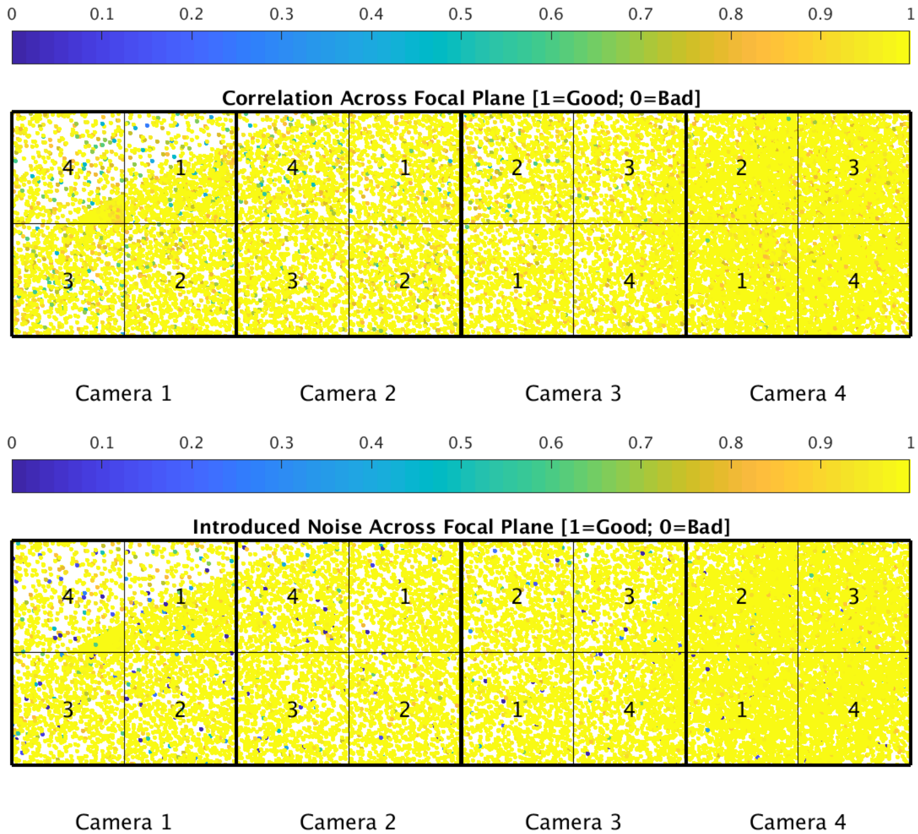


Figure 5: PDC residual correlation goodness metric (top panel) and PDC introduced noise goodness metric (bottom panel). The metric values are shown on a focal plane map indicating the camera and CCD location of each target. The correlation goodness metric is calibrated such that a value greater than 0.8 means there is less than 10% mean absolute correlation between the target under study and all other targets on the CCD. The introduced noise metric is calibrated such that a value greater than 0.8 means the power in broad-band introduced noise is below the level of uncertainties in the flux values.

The vertical histogram in the right panel of Figure 7 shows the distribution of transit depths derived from limb-darkened transiting planet model fits for TCEs. The model transit depths range down to the order of 100 ppm, but the bulk of the transit depths are considerably larger.

A search for additional TCEs in potential multiple planet systems was conducted in DV through calls to TPS. A total of 1475 TCEs were ultimately identified in the SPOC pipeline on 1021 unique target stars. Table 4 provides a breakdown of the number of TCEs by target. Note that targets with large numbers of TCEs are likely to include false positives.

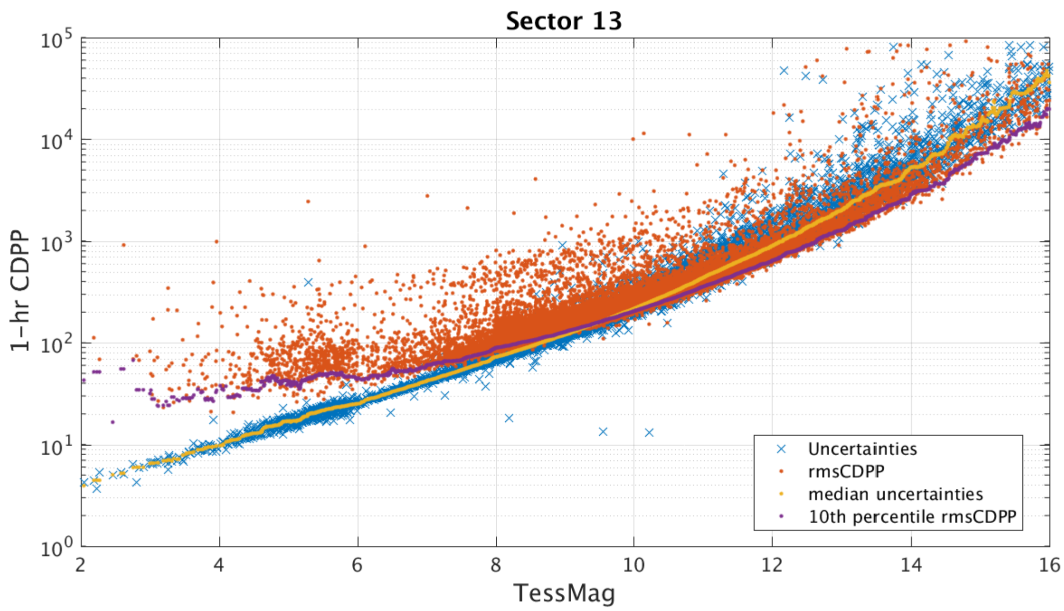


Figure 6: 1-hour CDPP. The red points are the RMS CDPP measurements for the 19997 light curves from Sector 13 plotted as a function of TESS magnitude. The blue x's are the uncertainties, scaled to 1-hour timescale. The purple curve is a moving 10th percentile of the RMS CDPP measurements, and the gold curve is a moving median of the 1-hr uncertainties.

Table 4: Sector 13 TCE Numbers

| Number of TCEs | Number of Targets | Total TCEs |
|---|---|---|
| 1 | 666 | 666 |
| 2 | 279 | 558 |
| 3 | 58 | 174 |
| 4 | 14 | 56 |
| 5 | 3 | 15 |
| 6 | 1 | 6 |
| – | 1021 | 1475 |

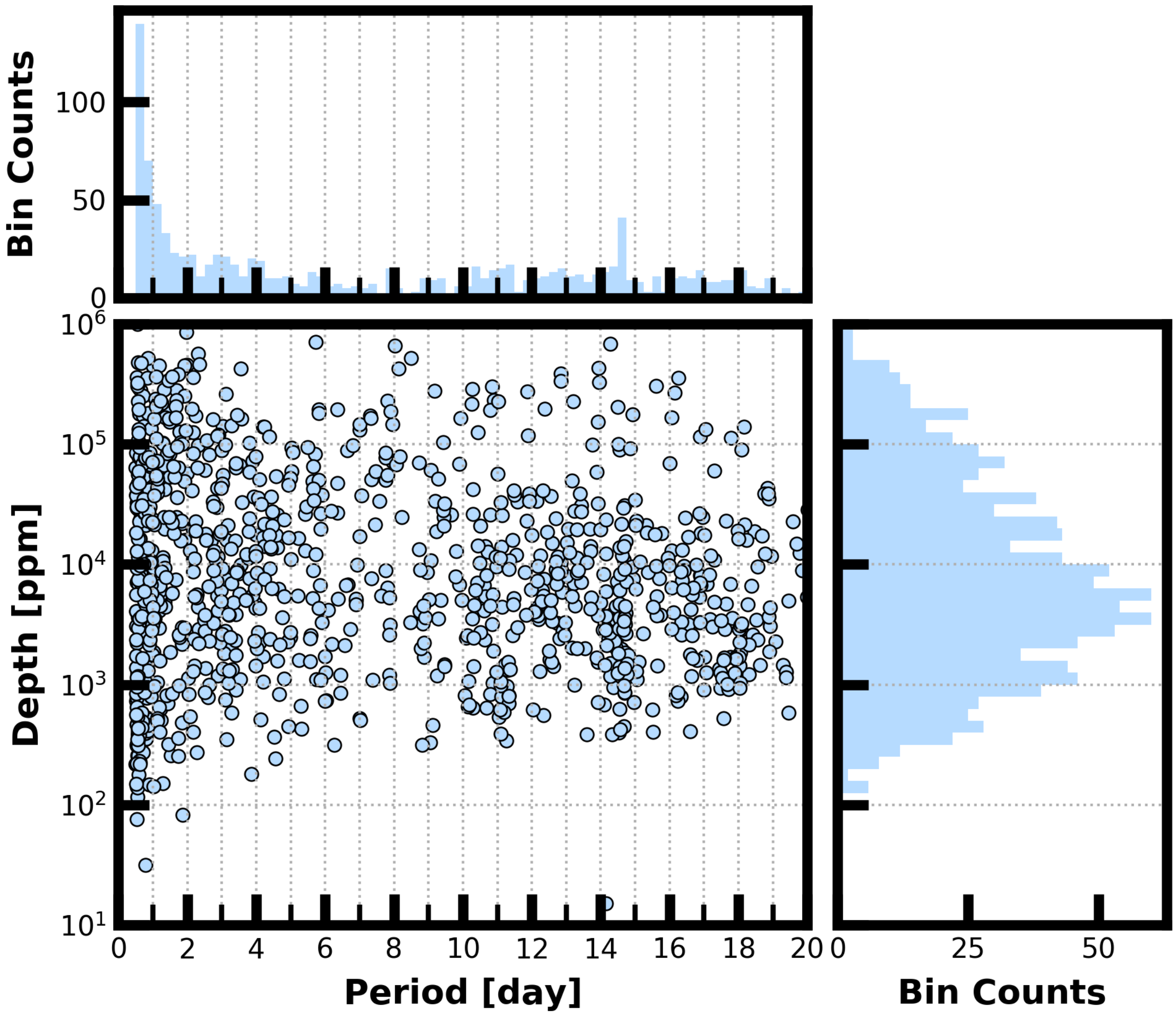


Figure 7: Lower Left Panel: Transit depth as a function of orbital period for the 1475 TCEs identified for the Sector 13 search. For enhanced visibility of long period detections, TCEs with orbital period <0.5 days are not shown. Reported depth comes from the DV limb darkened transit fit depth when available, and the DV trapezoid model fit depth when not available. Top Panel: Orbital period distribution of the TCEs shown in the lower left panel. Right Panel: Transit depth distribution for the TCEs shown in the lower left panel.

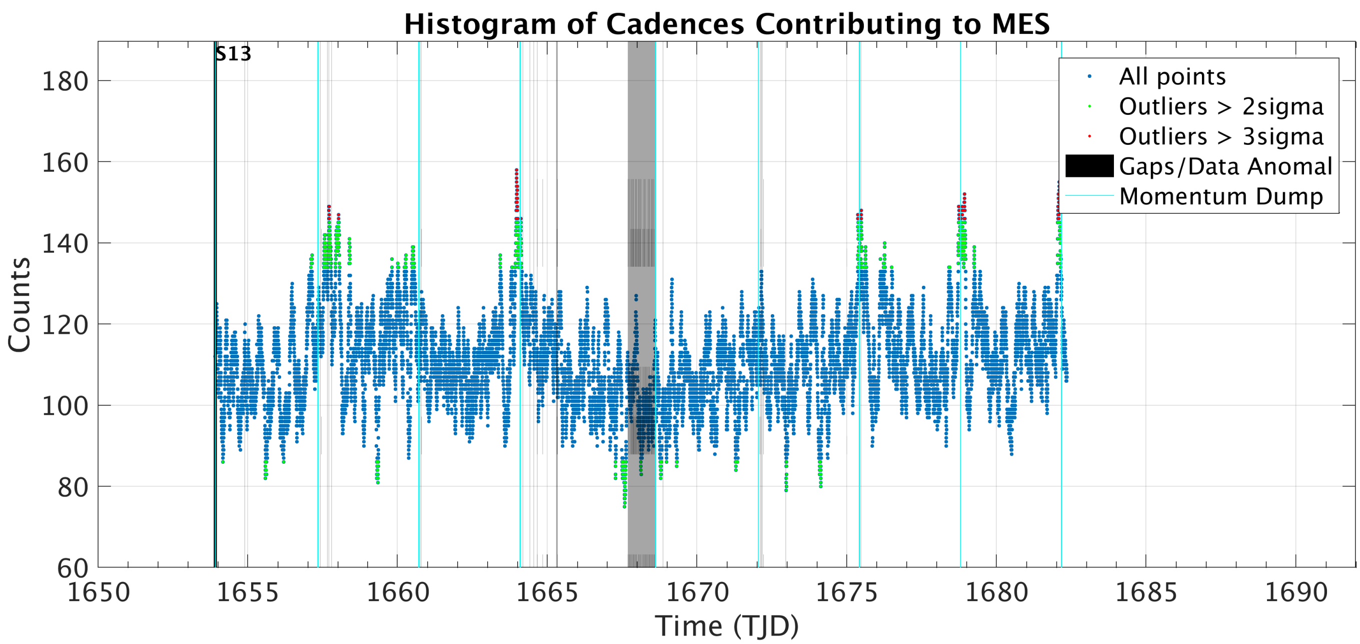


Figure 8: Number of TCEs at a given cadence exhibiting a transit signal. Isolated peaks are caused by a single event and result in spurious TCEs. The peaks typically align with pointing instabilities and strong background variations.

# References

Jenkins, J. M. 2017, Kepler Data Processing Handbook: Overview of the Science Operations Center, Tech. rep., NASA Ames Research Center

Jenkins, J. M., Twicken, J. D., McCauliff, S., et al. 2016, in Proc. SPIE, Vol. 9913, Software and Cyberinfrastructure for Astronomy IV, 99133E

Li, J., Tenenbaum, P., Twicken, J. D., et al. 2019, *PASP*, 131, 024506

Twicken, J. D., Catanzarite, J. H., Clarke, B. D., et al. 2018, *PASP*, 130, 064502

Vanderspek, R., Doty, J., Fausnaugh, M., et al. 2018, TESS Instrument Handbook, Tech. rep., Kavli Institute for Astrophysics and Space Science, Massachusetts Institute of Technology

# Acronyms and Abbreviation List

**BTJD** Barycentric-corrected TESS Julian Date

**CAL** Calibration Pipeline Module

**CBV** Cotrending Basis Vector

**CCD** Charge Coupled Device

**CDPP** Combined Differential Photometric Precision

**COA** Compute Optimal Aperture Pipeline Module

**CSCI** Computer Software Configuration Item

**CTE** Charge Transfer Efficiency

**Dec** Declination

**DR** Data Release

**DV** Data Validation Pipeline Module

**DVA** Differential Velocity Aberration

**FFI** Full Frame Image

**FIN** FFI Index Number

**FITS** Flexible Image Transport System

**FOV** Field of View

**FPG** Focal Plane Geometry model

**KDPH** Kepler Data Processing Handbook

**KIH** Kepler Instrument Handbook

**KOI** Kepler Object of Interest

**MAD** Median Absolute Deviation

**MAP** Maximum A Posteriori

**MAST** Mikulski Archive for Space Telescopes

**MES** Multiple Event Statistic

**NAS** NASA Advanced Supercomputing Division

**PA** Photometric Analysis Pipeline Module

**PDC** Pre-Search Data Conditioning Pipeline Module

**PDC-MAP** Pre-Search Data Conditioning Maximum A Posteriori algorithm

**PDC-msMAP** Pre-Search Data Conditioning Multiscale Maximum A Posteriori algorithm

**PDF** Portable Document Format

**POC** Payload Operations Center

**POU** Propagation of Uncertainties

**ppm** Parts-per-million

**PRF** Pixel Response Function

**RA** Right Ascension

**RMS** Root Mean Square

**SAP** Simple Aperture Photometry

**SDPDD** Science Data Product Description Document

**SNR** Signal-to-Noise Ratio

**SPOC** Science Processing Operations Center

**SVD** Singular Value Decomposition

**TCE** Threshold Crossing Event

**TESS** Transiting Exoplanet Survey Satellite

**TIC** TESS Input Catalog

**TIH** TESS Instrument Handbook

**TJD** TESS Julian Date

**TOI** TESS Object of Interest

**TPS** Transiting Planet Search Pipeline Module

**UTC** Coordinated Universal Time

**XML** Extensible Markup Language